(This is a sample cover image for this issue. The actual cover is not yet available at this time.)

Deep-Sea Research I 69 (2012) 51–61

Contents lists available at SciVerse ScienceDirect

Deep-Sea Research I

journal homepage: www.elsevier.com/locate/dsri

Large-scale sediment redistribution on the equatorial Pacific seafloor

Nathalie Dubois *[,1], Neil C. Mitchell

School of Earth, Atmospheric and Environmental Sciences, The University of Manchester, Oxford Road, Manchester M13 9PL, UK

ARTICLE INFO

Article history:
Received 31 March 2012
Received in revised form
8 July 2012
Accepted 17 July 2012
Available online 27 July 2012

Keywords:
Equatorial Pacific
Sediment
Focusing
Contourite
Seismic reflection

ABSTRACT

Understanding if and how particles are laterally transported before final deposition is crucial for accurately reconstructing paleoceanographic conditions from pelagic sediments. We use digital seismic reflection data from the AMAT03 site survey cruise for IODP EXP 320/321 to investigate the Neogene and Quaternary pelagic sedimentation across the eastern-central equatorial Pacific (110–130°W). Spatially continuous stratigraphy was derived from five latitudinal seismic transects between the Clipperton and Galapagos Fracture Zones, revealing evidence of widespread sediment redistribution increasing towards the western part of this region. A large-scale anomaly in sediment thickness in the northwestern part of the surveyed area suggests that sediment focusing and/or bottom-current induced resedimentation has been occurring in the central Pacific on timescales of millions of years. The relatively confined character of this anomaly does not support a longitudinally continuous focusing of sediments on the equator, as has been suggested to occur during the Pleistocene glacial stages.

1. Introduction

In paleoceanography, chemical and physical properties of sediments as well as their organic and inorganic constituents are used to reconstruct past environmental conditions. The sedimentation processes itself, however, is often neglected in those studies, based on the assumption that erosion and transport only marginally distort the original environmental record. The fact that paleoceanographers often look for basins or drifts that have unusually high sedimentation rates to extract high-resolution time series (e.g., Peterson et al., 2000; McManus et al., 1999) jeopardizes the basic supposition that pelagic and hemipelagic sediments are deposited by slow vertical sedimentation producing layers of sediment that uniformly drape the seafloor (Menard, 1964). Indeed, recent studies have shown that significant amounts of sediment in specific pelagic deposits do not reflect the surface environment directly above but may have traveled horizontally more than 1000 km (e.g. Ohkouchi et al., 2002; Mollenhauer et al., 2005). Such deposits therefore integrate an environmental signal over substantial lateral distances and can leave microfossils out of stratigraphic sequence (Thiede, 1981).

The equatorial Pacific is a prime target for paleoceanographic studies, as it is an important cog of Earth's climate, being a significant modulator of CO_2 exchanges with the atmosphere and representing more than half of the tropical oceans, the heat engine of the climate system. In the Pacific, constant-flux proxies such as excess ^{230}Th and extraterrestrial ^{3}He have been interpreted as evidence that significant lateral advection of pelagic material occurs in the water column or near the seabed, leading to marked spatial variations in deposition rates and in particular, to focusing of deposits on the equator (Higgins et al., 1999; Marcantonio et al., 2001; Mitchell and Lyle, 2005). Sediment focusing by currents within the water-column produces unrepresentative accumulation rates and sediment composition with respect to the biogenic production rates and particle composition in the immediately overlying surface water. As focusing does not involve erosion, mixing of fossil of different ages does not occur. On the other hand, when seafloor erosion by bottom currents and redeposition of the resuspended pelagic sediment on contourites is responsible for high accumulation rates, mixing of microfossils of different ages may occur. Contourites are defined as sediments deposited or significantly affected by bottom currents (Stow et al., 2002; Rebesco, 2005), where bottom current is any persistent water current near the seafloor. This distinguishes them from continuous vertical settling—the so-called background processes (pelagites and hemipelagites, Stow et al., 2008).

Quantifying the extent of lateral movement, whether in the water column or on the seafloor, has proven difficult and gave rise to an ongoing debate (e.g., Lyle et al., 2005; François et al., 2007). Large differences in sediment accumulation estimates have been obtained from two different methods to calculate sedimentation rates. Sediment ^{230}Th and ^{3}He radiometric data suggest that significant lateral sediment transportation occurs (François et al., 2004; Kienast et al., 2007). Much of the equatorial Pacific has a focusing factor (excess ^{230}Th accumulation relative to its

* Corresponding author. Tel.: +1 508 289 3418; fax: +1 508 457 2187.
E-mail address: ndubois@whoi.edu (N. Dubois).
[1] Now at Woods Hole Oceanographic Institution, MS#23, Woods Hole, MA 02543, USA.

0967-0637/$ - see front matter © 2012 Elsevier Ltd. All rights reserved.
http://dx.doi.org/10.1016/j.dsr.2012.07.006

water-column production) of >1, in places reaching >8, indicative of increased particle flux into particular sites by lateral advection (Higgins et al., 1999; Marcantonio et al., 2001; Loubere et al., 2004). On the other hand, mass accumulation rates – the mass of sediment that has accumulated between dated sediment horizons – suggest that such high levels of sediment focusing did not occur (Lyle et al., 2005, 2007).

Most of the evidence for large-scale horizontal sediment transport is based on geochemical measurements, which could also reflect, for instance, the scavenging of ^{230}Th and clay by the rain of organic matter (Higgins et al., 1999; Broecker, 2008). Moreover, the bottom currents responsible for sediment convergence at the seafloor have only been studied sporadically in limited locations (e.g. Johnson and Johnson, 1970), and sediment deficient regions serving as sources of winnowed sediments have not yet been clearly identified (Higgins et al., 1999). Thus there is a need for a more integrated approach to study the equatorial sedimentary system (Mitchell et al., 2003).

Drilling sites, which are often positioned in areas of locally enhanced deposition, may not be representative of the regional pattern of sedimentation. Previous seismic studies have revealed a rather patchy character of deposition attributed to spatially heterogeneous carbonate dissolution (Mitchell and Lyle, 2005). Areas alternately received an anomalous excess or deficit of sediment with length scales of 100 km. These central Pacific data do not show much evidence for the simple linearly increasing dissolution with depth, as in the classical carbonate dissolution model, in which carbonate mass accumulation rates (MARs) vary linearly with depth from a carbonate lysocline down to the Carbonate Compensation Depth (CCD) (Berger et al., 1982; Peterson, 1966). Above the lysocline, carbonate MARs are relatively unaffected by differences in depth, whereas below the CCD the sediments are carbonate free. The depths of both of these surfaces vary spatially and in time as a result of climatic and physical processes (Lyle, 2003). World Ocean Circulation Experiment observations have revealed significant topography in the carbonate saturation horizon for the Pacific, in particular three-dimensional complexity as the horizon shallows from the Antarctic Bottom Water in the south to the more corrosive Pacific Deep Water in the north (Feely et al., 2002, 2004). Based on the depth of the topmost transparent layer, Tominaga et al. (2011) identified the CCD at a depth of 4440 m. The modern regional CCD in the vicinity of the AMAT03 track had been previously identified between 4400 and 4800 m (Farrell and Prell, 1989; Berger et al., 1976). During most of the Paleogene the CCD was between 500 and 1300 m shallower than today, with some large short-term fluctuations (Lyle et al., 2005). A dramatic deepening of the Pacific CCD occurred during the Eocene–Oligocene transition from greenhouse to icehouse (van Andel et al., 1975). The CCD of the Neogene was much more stable, located near a depth of 4500 m, but also fluctuated. Intervals of lower carbonate deposition in the eastern equatorial Pacific have been interpreted as changes in the CCD depth (at ~18 and ~10 Ma) (Lyle et al., 1995; Lyle, 2003). On the other hand, the role of carbonate dissolution versus elevated deposition of biosilica still needs to be determined.

Here we use digitally acquired seismic reflection records to reexamine pelagic sedimentation in the eastern-central equatorial Pacific with the aim of documenting large-scale processes.

2. Background

Surface divergence and upwelling of nutrient-rich subsurface water enhance primary productivity within a 2° latitudinal band of the equator, leading to higher sedimentation rates that have formed a sediment bulge on the seafloor (Ewing et al., 1968). The bulge consists of a few hundred meters of biogenic sediments, composed mostly of calcium carbonate and siliceous planktonic remains, but very little clay (van Andel and Moore, 1974). It is skewed to the north of the equator because of the northwestward movement of the Pacific Plate (Koppers et al., 2001; Mitchell et al., 2003). The thickest part of the equatorial sediment bulge, reaching almost 600 m, is in the central Pacific around ~140°W. It is located on ~50 Ma old crust, which has had sufficient time to collect sediment since it was created at the East Pacific Rise, but has not yet cooled and sank enough (i.e. below the CCD) for the carbonate sediments to be strongly dissolved as occurs further west (Knappenberger, 2000).

Mayer et al. (1985a) published the first major investigation into the seismic stratigraphy of the equatorial sediments, in the central Pacific (134°W). They identified reflectors associated with changes in carbonate content in the sediments drilled at DSDP Site 574 (Fig. 1). Calcium carbonate ($CaCO_3$) has a higher density than most other sediments being deposited, in particular it has a lower porosity and higher grain density than biosiliceous sediments (Mayer, 1991), therefore, any significant shift in the ratio of $CaCO_3$:SiO_2 causes a change in density and acoustic impedance, creating a seismic horizon. Mayer et al. (1985a, 1986) proposed that these impedance contrasts were chronostratigraphic, caused by major paleoceanographic changes in deposition and/or dissolution of calcium carbonate. Mayer et al. (1985a, 1986) defined 8 regionally traceable reflectors spanning 25 Ma of deposition, which they named with color designations: Green, Magenta,

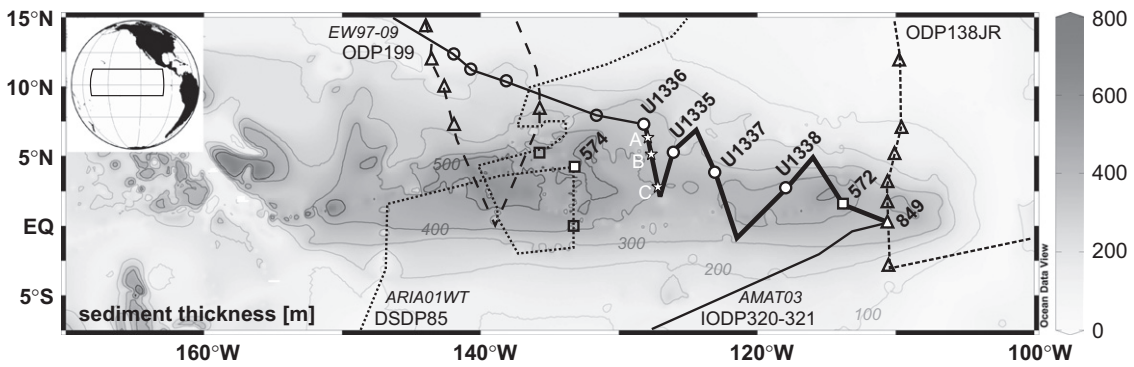

Fig. 1. Tracklines of various cruises having acquired digital seismic reflection data in the central Pacific (*Ariadne-1* (ARIA01WT) for DSDP85, *Ewing* (EW97-09) for ODP199, AMAT03 for IODP 320–321, ODP138JR), shown on a map of sediment thickness (Divins, 2012). IODP drillsites are indicated by circles, DSDP sites are shown by squares and ODP sites are shown by triangles. White symbols indicate sites used for ground truth, whereas open symbols show location of drill site not used in this study. A thicker line highlights the segment of the AMAT03 site survey cruise analyzed in this study. Stars A–C locate erosion features discussed in the text and shown in Fig. 5.

Brown, Purple, Red, Lavender, Yellow, and Orange. At least two of these reflectors were identified in the eastern equatorial Pacific at 110°W, in sediments recovered by ODP Leg 138 (Bloomer et al., 1995), >2000 km east of DSDP Site 574, while six of these reflectors were identified further west, in sediments recovered by ODP Leg 199 around 140°W (Mitchell et al., 2003), providing support for their chronostratigraphic nature (Fig. 1, see cruise track ODP138JR and EW97-09, respectively). At 110°W, the reflectors are also generated by compositional changes associated with abrupt deposition of more siliceous sediments (Bloomer et al., 1995), so ties to scientific drilling data are needed for confirmation.

This study focuses on the seabed and basement reflectors in order to compute sediment thickness over a region more than 3000 km across. Previous investigations of the equatorial bulge have not always been able to identify the basement (e.g., Mitchell et al., 2003). Using Mayer et al.'s (1985a) reflectors and ties to stratigraphy at scientific drilling sites we also mapped out the large-scale carbonate stratigraphy across a major part of the equatorial sediment bulge, connecting previous work at 110°W (Bloomer et al., 1995) to earlier studies around 135°–140°W (Mayer et al., 1985a, 1986; Mitchell et al., 2003).

3. Material

3.1. Seismic data

Multichannel seismic reflection, multibeam echosounder and chirp sonar data were collected during the AMAT03 cruise (March–April 2004) on R/V *Revelle*. Data are archived at the Marine Geoscience Data System UTIG portal (http://www.ig.utexas.edu/sdc/cruise.php?cruiseIn=amat03rr). The AMAT03 cruise was designed as a site survey for IODP Exp 320/321: the Pacific Equatorial Age Transect (PEAT) drilling program. This program was developed to understand how a major oceanic region evolved over the Cenozoic Era (65–0 Ma), drilling a series of sites that originated on the paleoequator (Lyle et al., 2010). The survey crossed 10–53 Ma seafloor and extends over the area between 150°W–110°W and 5°S–15°N (Fig. 1).

A 4-channel Sercel streamer was towed at ~10 knots during underway surveys and a 48-channel Geometrics GeoEel streamer was towed at ~6 knots at most of the PEAT site surveys. The seismic sources were two 150 c.i. generator/injector (GI) guns fired at 10 s intervals for both 4- and 48-channel operations. Data were recorded with a 0.5 milliseconds (ms) sampling interval and 8 s record length. No analog high- or low-cut filter was applied during recording.

We used ~4740 km from the original ~6145 km total track-length of seismic data. We focused on 96 segments of the underway seismic reflection profiles to study large-scale sediment deposition and redistribution. Survey segments at sites U1335, U1336, U1337 and U1338 were used to ground truth the interpreted reflectors, in addition to underway profiles crossing Sites DSDP 572 and ODP 849 (Fig. 1).

3.2. IODP data

3.2.1. Drill sites

The correspondence between AMAT03 site survey names and the IODP drilling sites used in this study are as follows: PEAT5 (Site U1336, 32 Ma crust), PEAT6 (Site U1335, 26 Ma crust), PEAT7 (Site U1337, 24 Ma crust), and PEAT8 (Site U1338, 18 Ma crust). The PEAT expedition biostratigraphy, physical and chemical property data (Pälike et al., 2010) confirm the Mayer et al. (1985a) seismic stratigraphy and tie the east Pacific seismic stratigraphy with that of the central Pacific.

3.2.2. Downhole Logging data

Wireline logging was conducted at U1337 and U1338. The three downhole logging tool strings deployed consist of a modified triple combo (without a neutron porosity measurement), a Formation MicroScanner (FMS)–sonic combination, and a Vertical Seismic Imager (VSI) seismic tool with a Scintillation Gamma Ray (SGT-N) sonde (Pälike et al., 2010). The modified triple combo and FMS–sonic tool strings recorded natural gamma-ray radioactivity, bulk density, electrical resistivity, elastic wave velocity, and borehole resistivity images. The VSI seismic tool string recorded seismic waveforms in a vertical seismic profile (VSP) experiment. No wireline logging was conducted at U1336, and only downhole temperature measurements were conducted at U1335.

3.2.3. Vertical seismic profile (VSP)

Full details of the VSP experiments carried out by A. Malinverno are given by Pälike et al. (2010). Briefly, in a VSP experiment, the VSI records the full waveform of elastic waves generated by a seismic source positioned just below the sea surface. A Sercel G. Gun Parallel Cluster (two 250 in.^{3} air guns separated horizontally by 1 m) was used as a seismic source. The recorded waveforms were stacked and a one-way traveltime was determined from the median of the first breaks for each station. These "check shot" measurements relate depth in the hole to traveltime in reflection seismic lines, allowing accurate correlation between well data (i.e. stratigraphic events) and seismic section (i.e. seismic reflectors).

Traveltime–depth relationships were constructed in both U1337 and U1338. To construct the relationship in U1337 (U1338, respectively), Pälike et al. (2010) started from the Two-Way Travel Time (TWTT) from sea level to the seafloor (5.9444 s, 5.5862 s), computed from the uncorrected seafloor depth measured by the *JOIDES Resolution's* echo sounder (4458.3 m, 4189.6 m). The difference between this time and the arrival time to the shallowest receiver in the VSP gives an average P wave velocity of 1514 m/s (1500 m/s) between the seafloor and 214.1 m (190.6 m) wireline log depth below seafloor (WSF). The dependence of the arrival times on depth in the VSP receiver array can be fit very closely by a second-degree polynomial:

$$\text{In } U1337: t(z) = 5.9414 + (1.4378 \times 10^{-3})z - (4.8984 \times 10 - 7)z^2,$$

$$\text{In } U1338: t(z) = 5.5796 + (1.5037 \times 10^{-3})z - (6.8064 \times 10^{-7})z^2,$$

where t is TWTT (s) and z is depth below seafloor ($214.1 \le z \le 438.8$ m WSF, $190.6 \le z \le 415.7$ m WSF). The maximum residual on this fit is 0.45 ms (1.7 ms) and the root-mean-square residual is 0.23 ms (0.94 ms).

The TWTTs obtained by *JOIDES Resolution's* echo sounder on IODP Expedition 329 (5.9444 s, 5.5862 s; see above) for U1337 and U1338 are more accurate than the TWTT estimated during the AMAT03 site survey cruise, and have therefore been used to reconstruct the traveltime–depth relationship at those site. The TWTTs of the reflectors given in Table 1 on the other hand reflect those observed in the AMAT03 seismic reflection lines.

4. Methods

We investigated the large-scale pelagic sedimentation regimes on 10–32 Ma ocean crust by using both new seismic interpretations from the AMAT03 site survey and the stratigraphy from DSDP, ODP and IODP drill sites in the equatorial Pacific.

Table 1
Statigraphic and seismic horizons depth at DSDP, ODP and IODP sites.

Horizon	TWTT (s)[a]	Depth (mbsl)	Age (Ma)
ODP 849B (0°10.983′N, 110°31.183′W) AMAT-03-jd077_2034, SP 11791			
Seafloor	5180	3839	0
Green	5344	3964	3.8–4.6
Magenta	5431	4033	5.2–6.2
Brown	5483	4076	8.3–8.38
Purple	5572	4151	9.6–10.5
Basement	5620	4192	12.5
DSDP 572 (1°26.09′N, 113°50.52′W)—AMAT-03-jd078_2000, SP 19974			
Seafloor	5185	3893	0
Green	5279	3964	3.8–4.6
Magenta	5315	3992	5.2–6.2
Brown	5410	4066	8.3–8.38
Purple	5529	4165	9.6–10.5
Basement	5743	4372[b]	15
Site U1338B (2°30.469′N, 117°58.174′W)—AMAT-03-PEAT8D line 1, SP 36015			
Seafloor	5621	4199	0
Green	5688	4249	3.8–4.6
Pliocene/Miocene		*4274*	*5.332*
Magenta	5737	4285	5.2–6.2
Brown	5790	4326	8.3–8.38
Purple	5926	4432	9.6–10.5
Late/mid-Miocene		*4447*	*11.61*
Red	6059	4556	13.5–15
Mid/early Miocene		*4563*	*15.97*
Lavender	6079	4576	15.7–17
Basement	6118	4615	18
Site U1337A (3°50.007′N, 123°12.356′W)—AMAT-03-PEAT7C line 4, SP 1756			
Seafloor	5989	4461	0
Green	6072	4524	3.8–4.6
Pliocene/Miocene		*4548*	*5.332*
Magenta	6122	4561	5.2–6.2
Brown	6180	4606	8.3–8.38
Purple	6224	4639	9.6–10.5
Late/mid-Miocene		*4691*	*11.61*
Red	6366	4755	13.5–15
Mid/early Miocene		*4791*	*15.97*
Lavender	6420	4803	15.7–17
Oligocene/Miocene		*4906*	*23.03*
Basement	6533	4910	24.5
Site U1335A (5°18.734′N, 126°16.995′W)—AMAT-03-PEAT6C line 8, SP 19103			
Seafloor	5819	4328	0
Green	5843	4346	3.8–4.6
Pliocene/Miocene		*4356*	*5.332*
Magenta	5859	4358	5.2–6.2
Brown	5879	4373	8.3–8.38
Purple	5894	4385	9.6–10.5
Late/mid-Miocene		*4406*	*11.61*
Red	6022	4487	13.5–15
Mid/early Miocene		*4488*	*15.97*
Lavender	6045	4506	15.7–17
Oligocene/Miocene		*4683*	*23.03*
Basement	6262	4748[c]	26
Site U1336A (7°42.067′N, 128°15.253′W)—AMAT-03-PEAT5C line 6, SP 42593			
Seafloor	5753	4285	12
Red	5783	4308	13.5–15
Mid/early Miocene		*4330*	*15.97*
Lavender	5816	4333	15.7–17
Oligocene/Miocene		*4435*	*23.03*
Basement	6070	4588[d]	32

[a] TWTT were computed as follows: U1337 and U1338 using velocity from respective VSP exepriments, ODP 849 and DSDP 572 from ODP 849 velocity profile, U1335 and U1336 from DSDP 574 velocity profile.
[b] DSDP 572: basement observed at 5743 ms, which using the ODP 849 velocities translates into an estimated sediment cover of 454 m, while the sediment–basement contact was encountered at 479.5 m during drilling.
[c] U1335: basement observed at 6262 ms, which using the DSDP 574 velocities translates into an estimated sediment cover of 363 m, while 420 m were recovered.
[d] No complete penetration during drilling, stopped at 303 mbsf (estimated at 253 m from seismic).

The seismic data were processed by band pass filtering, normal move-out, stacking, and F-K migration (details available http://www.ig.utexas.edu/sdc/cruise.php?cruiseIn=amat03rr).

For consistency with earlier work, we identified and mapped the same reflectors as Mayer et al. (1985a). Comparing $CaCO_3$ profiles from Site DSDP 572, DSDP 574, ODP 849 and IODP

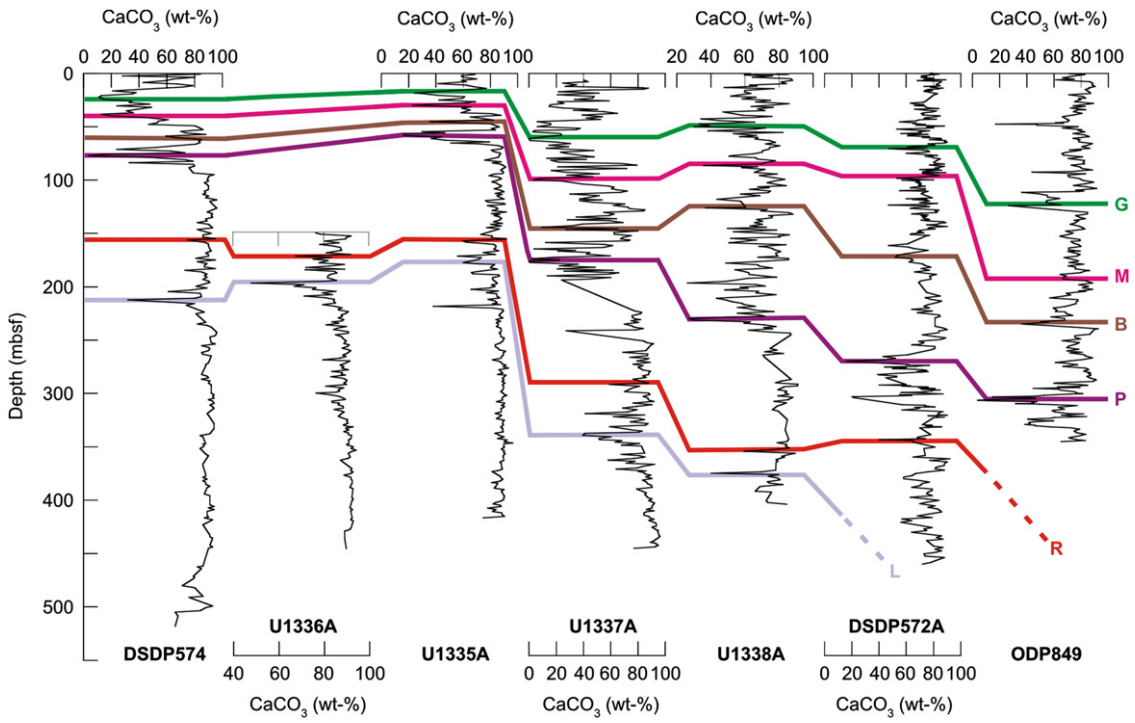

Fig. 2. Down-core $CaCO_3$ profiles at six drill sites crossed by our seismic survey, correlated to the $CaCO_3$ profile of DSDP 574, used by Mayer et al. (1985a) for the construction of the first seismic stratigraphy of the Pacific equatorial bulge. Reflectors are identified by their respective color nomenclature of Mayer et al. (1985a) (green—G, magenta—M, brown—B, purple—P, red—R, lavender—L). Note that site U1336A has been shifted down by 150 m to facilitate the visualization. (For interpretation of the references to color in this figure legend, the reader is referred to the web version of this article.)

U1335–U1338 was particularly useful to recognize the correlative paleoceanographic events first recognized in Site 574 and their corresponding reflectors (Fig. 2 and Table 1, Supplementary Fig. A1). We also made use of the biostratigraphy developed during IODP Exp 320/321 to constrain the depth of these horizons (Table 1; Pälike et al., 2010).

We used four prominent features in our seismic profiles for our interpretation: the basement reflector, the Purple and Lavender horizons as identified by Mayer et al. (1985a), and the seafloor reflector. The ages of these reflectors (Purple: 9.6–10.5 Ma, Lavender: 15.7–17 Ma) were recently revised to account for more recent biostratigraphy and magnetostratigraphy (Mitchell et al., 2003). The Purple horizon is associated with an extremely large carbonate minimum that results in a large impedance contrast (Mayer et al., 1985a). It is the main dissolution interval, traceable throughout much of the eastern equatorial Pacific where drillsites have a Miocene carbonate section. The Lavender reflector, on the other hand, correlates with a large carbonate minimum, the "Chron 16 carbon shift". In terms of paleoceanographic events, Mayer et al. (1986) correlated the Purple reflector with the intensification of North Atlantic bottom water circulation, whereas they suggested the Lavender reflector represents an intensification of Antarctic Bottom Water Circulation and the partitioning of silica between the Atlantic and the Pacific. These two reflectors correspond to short-term deepenings of the CCD (see paragraph 1 above).

Using these four prominent reflectors as distinctive markers, we interpreted sediment intervals between ~1°S–7°N and ~110W°–128°W. We separated the data into 5 latitudinal transects, in order to address North–South and East–West trends in productivity, dissolution, sediment transport and deposition (Fig. 3). Seismic TWTT data have been smoothed to reduce fluctuations using a simple boxcar filter of different full width: 1°, 0.5° and 0.1° of latitude.

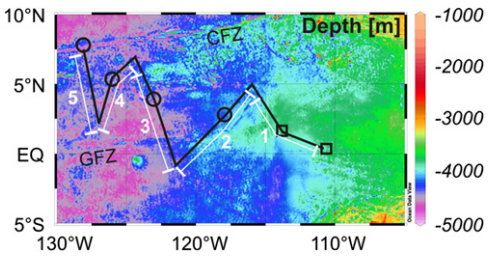

Fig. 3. Bathymetric map showing the 5 latitudinal transects (white lines and numbers). IODP sites (black circles) and DSDP/ODP sites (black squares) are also given (see details in Fig. 1). The Clarion Fracture Zone (CFZ) and the Galapagos Fracture Zone (GFZ) can be distinguished. Data from Smith and Sandwell (1997).

5. Results

The seafloor in the central Pacific is characterized by a few seamounts, a series of abyssal hills and basins, and minor late stage faulting in the basement. This basement faulting is particularly visible in the easternmost Transect 1 (not shown). The origin of the late stage faults is not known and might result from multiple causes, such as extended deforming plate boundary or cracking lithosphere (see review by Tominaga et al., 2011). The abyssal hills were formed at the fast spreading East Pacific Rise and have a typical height of ~400 m (measured from the seismic profile) whereas the abyssal basins have a typical width of ~10 km. The bathymetry deepens from east to west (Fig. 3).

The distribution of seismic horizons in the central Pacific is constrained by younger basement to the east and by preservation of biogenic sediments to the north. As a result, the full stratigraphic sequence is almost never present at any given location

(see Figs. 2 and A1). The older reflectors (> 18 Ma) disappear to the east because of the basement getting younger, whereas the more recent reflectors cannot be found to the north because of the increasing age of biogenic sediments immediately below the surficial red clay due to the northward movement of the Pacific Plate. The Brown and Purple horizons can be correlated over the entire extent of our survey, which represents 18° in longitude and 8° in latitude, whereas the Green and Magenta reflectors disappear northward around 5°N, and the Lavender and Red reflectors cannot be traced east of U1337, although they can be distinguished in the carbonate content at the drill sites (Fig. 2). The thickness of the units observed in the seismic records reflect this pattern, with thicker younger units in the southeast and thicker, older units in the northwest (Fig. A1).

Using a constant velocity of 1500 m/s, we made a rough first-approximation of the overall thickness of the sediment cover in the area surveyed, estimated to range between 300 m and 600 m (200–400 ms). Based on the VSP data (Pälike et al., 2010), a maximum uncertainty of ±5% is expected from our constant velocity assumption. Sediment cover appears to be absent from prominent hills, while the thickest cover (560 ms) is found close to DSDP Site 572, where the sediment–basement contact was reached at 479.5 mbsf during drilling. The general trend in sediment cover is as expected, conforming to the geographic dimensions of the equatorial sediment mound and thinning to the north away from the equator (Fig. 4, van Andel et al., 1975; Mitchell, 1998; Mitchell et al., 2003). However, one notable exception occurs in the northwestern part of the surveyed area: The seismically determined sediment thickness reveals an area of great sediment thickness in Transect 5, the westernmost line, north of 4.5°N. The site survey data (Lyle et al., 2006; Pälike et al., 2008) show that Site U1336, at the north end of this line, is on abyssal hill topography draped with thick sediment. This transect is the only one showing a significant northward thickening of the sediment cover. In Fig. 4, we added two latitudinal transects from previous work (Mitchell et al., 2003) to the west of our area (*EW97-09* in Fig. 1), which exemplify the expected northward thinning of the sediment cover.

6. Discussion

6.1. Sediment surplus

Ocean crust beneath every IODP Exp 320/321 site was formed at the East Pacific Rise at a latitude of ~1–2°S and has since been carried to the northwest by Pacific plate movements (see Fig. 1B in Lyle et al. (2010)). As a result, the upper part of the sedimentary section at each site is expected to have significantly slower sedimentation rates, reflecting the fact that the site left the equatorial zone of high sediment flux to the seafloor. The four sites in our study remained within the equatorial zone (±2° of the equator) for 15–18 m.yr., except U1336, which was formed slightly to the north of the equator (~1°N) and therefore only remained 8 m.yr. within the equatorial zone (Lyle et al., 2010). The excess sediment in the northern half of Transect 5, in the vicinity of U1336, can therefore with difficulty be accounted for solely by high equatorial productivity. In addition, the linear sedimentation rate recorded at U1336 during its time in the equatorial zone (15 m/Myr) is slightly lower than those recorded at the other sites from our study (25 m/Myr for U1335, 21 m/Myr for U1337 and 28.7 m/Myr for U1338). Even more surprisingly, the sedimentation rate at U1336 does not reveal a large decrease after it left the equatorial zone (see Fig. 5 in Lyle et al., 2010), as occurs at Sites U1335, U1137 and U1338, again providing no evidence for a productivity-driven excess sediment deposition.

Care must be taken, however, as the sediment surplus is located south of the Clipperton Fracture Zone (CFZ) on ~28 Ma old crust, whereas U1336 is located ~30 km north of the CFZ, on 32 Ma old crust. On the other hand, the site survey shows that U1336 is also thickly covered with sediment (300–400 ms TWTT). The total sediment thickness, using the velocity–depth conversion for DSDP Site 574 (Mayer et al., 1985a) was estimated as 253 m prior to drilling. Coring at this site stopped at 302.9 m core depth below seafloor (CSF), before reaching the basement. Thus the interval velocities published for DSDP Site 574 underestimate the basal interval velocities and therefore total sediment thickness (note that the same occurs at U1335, and at Site DSDP 572 using

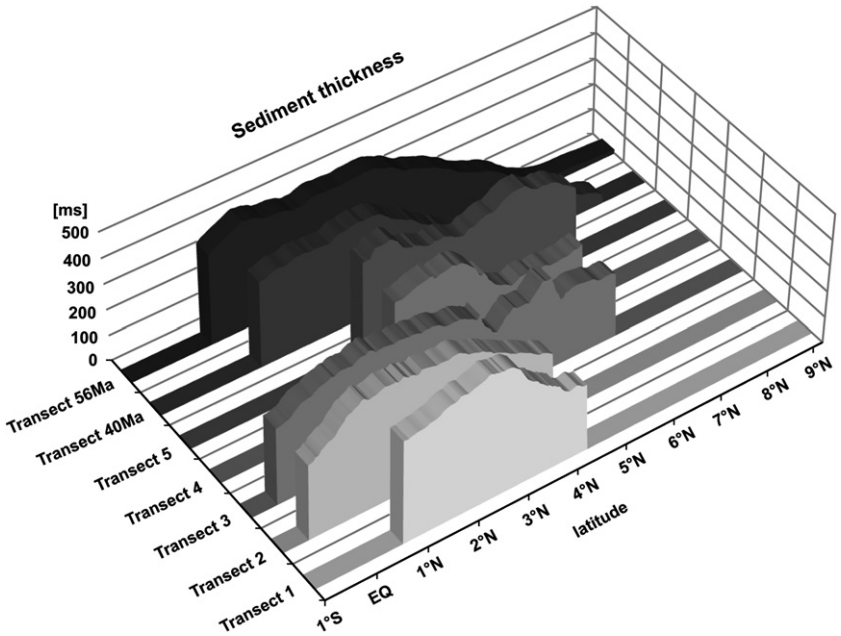

Fig. 4. Sediment thickness in TWTT (ms) along Transects 1–5 in addition to the two EW97-09 transects (40 and 56 Ma lines (Mitchell et al., 2003)). As basement was not recognized in the EW97-09 study, the thickness of those lines is taken as the sediment interval between the seafloor and the deepest (Yellow, 19.7–20.5 Ma) reflector. All data have been smoothed with a simple boxcar filter of full width 1° of latitude.

the ODP 849 velocity profile, see Table 1). Although gravity flow deposits have been observed to add to the sediment column at Site U1336 (Pälike et al., 2010), these flows would not affect the excess sediment interval located south of the CFZ, as they would need to cross the roughly 1000 m deeper trough in the fracture zone. Water depth in the vicinity of U1336, between 4200 and 4400 m, is relatively shallow for the age of the crust. The crust south of the CFZ is only 100 m deeper than the crust north of the zone, despite a water depth of nearly 5 km in the middle of the fracture zone trace. The relatively shallow depth could partly explain the thick deposits due to lower dissolution rates. But the modern lysocline in the eastern tropical Pacific west of the East Pacific Rise is about 3.5 km (Lyle et al., 1995), so carbonates are being dissolved at the seafloor in all our transects. The latitude-dependent decrease in $CaCO_3$ production away from the equator is an important defining factor of the regional CCD, which shallows away from the equatorial region (Lyle, 2003). Thus, variations in the depth of the CCD and in the latitudinal extent of carbonate production throughout the Neogene (Lyle, 2003) would have led to stronger dissolution in the northern and western part of our studied area, i.e. transect 5 where excess sediment is observed.

The presence of numerous indicators of erosion in Transect 5 lead us to suggest that resuspension and redeposition by bottom current is the main factor for the unusually thick sediment cover here. Examples of recent erosion and reworking

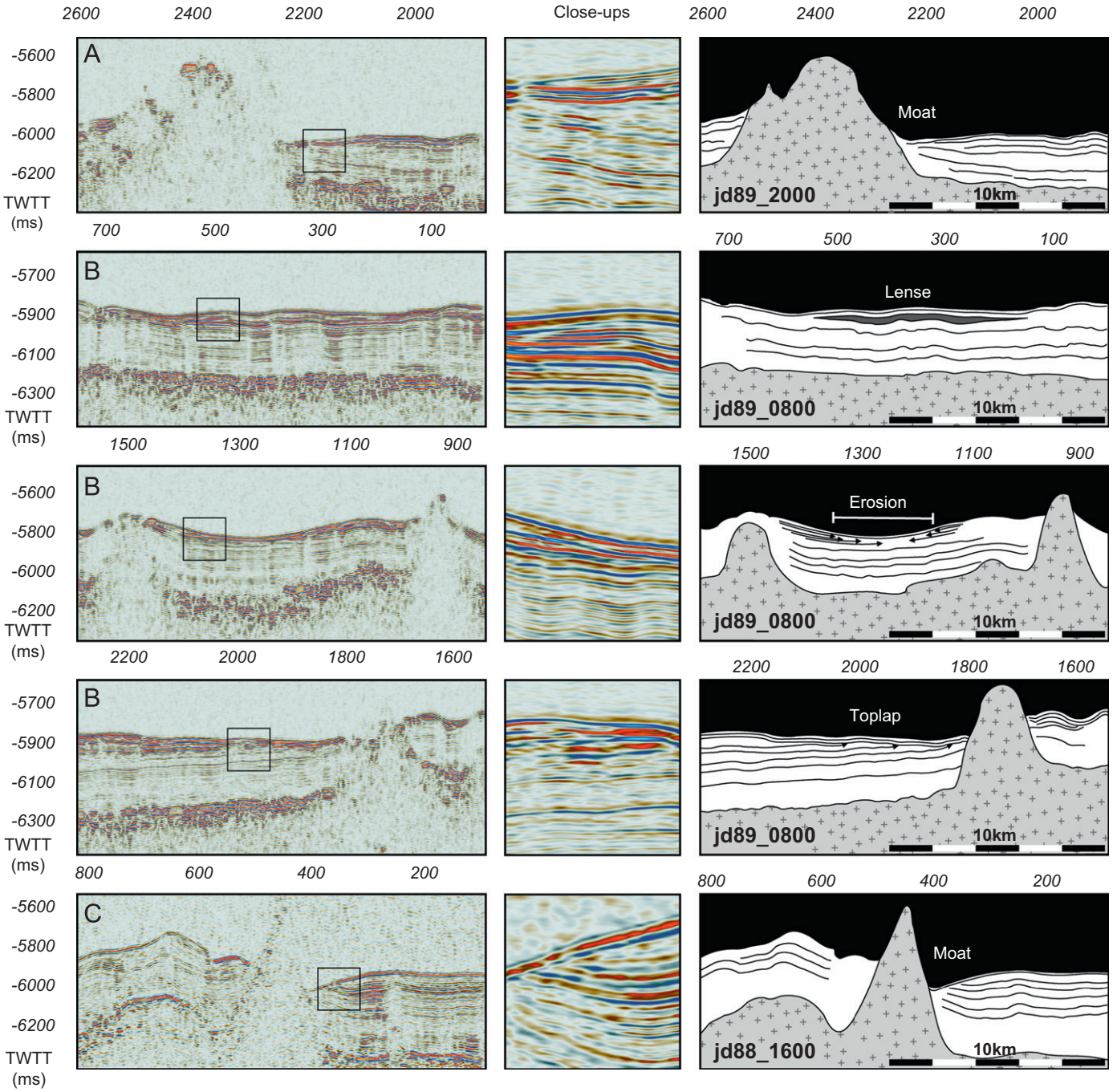

Fig. 5. Erosional features observed in Transect 5. Letters A–C refer to the stars located in Fig. 2. Numbers at the top of the panels refer to seismic trace numbers. Left column: Original seismic lines. Squares show locations of the close-ups (middle column, at 400% of the original seismic line). Right column: Seismic interpretation drawings, with line names. A tuning effect can be observed on both extremities of the lens in B (top).

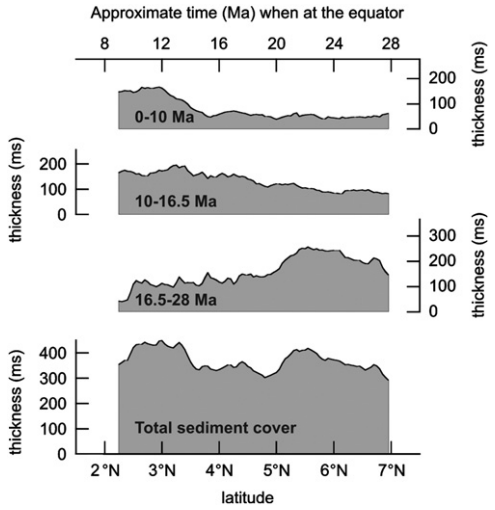

Fig. 6. Sediment thickness in TWTT (ms) along Transect 5 plotted versus latitude for various time intervals. Data have been smoothed with a simple boxcar filter of full width 0.5° of latitude. 0–10 Ma corresponds to the sediment thickness between the seafloor and Purple reflector, 10–16.5 Ma to the interval between the Purple and Lavender reflectors, 16.5–28 Ma to the interval between the Lavender reflector and the Basement. The total thickness of the sediment cover is given in the lower panel. The approximate age (assuming 0.25°/Myr northward movement, see Koppers et al., 2001) at which the paleo-equator was located at the modern sediment latitudes shown is given at the top of the figure.

features in Transect 5 are illustrated in Fig. 5, in particular erosional moats at the base of hills, truncations (top laps) and sediment lenses. These seismic profiles show that substantial erosion and redeposition occurred relatively recently in geologic time in this area. The large-scale sediment anomaly, on the other hand, has mostly been deposited at an earlier time (Fig. 6). Using Mayer et al.'s (1985a) stratigraphy clearly indicates that the excess sediment has been deposited before 16.5 Ma (i.e. the Lavender horizon). Although this interval does correspond to the time when the seafloor at this latitude was located at the paleo-equator (see Fig. 6), we dismiss higher equatorial productivity as the sole factor for the excess sediment as adjacent Transect 4 of similar basement age does not reveal such thick sediment deposits at similar latitude (Fig. 4). We thus suggest that, if strong equatorial sediment focusing was already occurring during the late Oligocene–early Miocene, it was not zonally continuous. Unfortunately the quality of the seismic profiles does not allow erosional features to be distinguished in the deepest part of the profile. Therefore, it would be difficult to distinguish between sediment focusing and bottom-current induced resedimentation as the main process responsible for this contourite-like deposit.

The mechanisms by which sediments are suspended and transported to a site of interest at the bottom of the ocean are still poorly known in the equatorial region. In keeping with reports of earlier workers (Johnson and Johnson, 1970; Shipley et al., 1985; François et al., 2004), we interpret the sediment as having been redistributed by advecting near-seafloor currents. Although a recent study by Tominaga et al. (2011) suggested that syndepositional sediment transport from abyssal hills to adjacent valleys is relatively small, large-scale lateral sediment transport in the central equatorial Pacific is supported by the following core-based evidence for winnowing and erosion as well as bottom current meter data. Seismic reflection data recovered during the ARIA01WT Expedition (Fig. 1), the site survey for DSDP Leg 85, reveal abundant evidence of recent seafloor erosion, such as erosional moats at the base of isolated highs or well-defined channels (Shipley et al., 1985). JGOFS piston core TT013-PC105 recovered at 5°N and 140°W contains Tertiary chalk below a depth of 2 m, with hiatuses or multiple erosional surfaces above, indicating removal of sediments by bottom currents (Marcantonio et al., 2001). Similarly, the uppermost sample investigated for biostratigraphy in U1336 indicates a Zone NN6 age (i.e. ~12 Ma). A bottom current meter installed at MANOP site C recorded a speed in excess of 10 cm/s during much of the year, with bursts exceeding 20 cm/s at a depth of 4400 m, 50 m above the bottom (Marcantonio et al., 2001). Critical erosion speeds reported vary from ~8 to 16 cm/s for the resuspension of the phytodetrital fluff layer (Beaulieu, 2003; Nodder et al., 2007) to 15–35 cm/s for pelagic carbonate silt (Southard et al., 1971).

Thiede (1981) suggested that strong erosional currents have been active in the western Pacific almost continuously for the past 15 Ma as well as during the interval 25–42 Ma, based on the presence of reworked microfossils in younger intervals. Biostratigaphic results from Site 574 on the other hand indicate periods of reworking from 4.7 to 0 Ma and from about 20 to 13 Ma (Mayer et al., 1985b), which coincides with the time of deposition of the excess sediment in Transect 5.

We hypothesize that deep-sea currents shaped the equatorial bulge, removing particles from the area centered at 125°W, where sediment cover only reaches 300 m (Fig. 1), and subsequently transported them to the contourite where excess sediment is observed farther north. This winnowing could explain the thinner sediment cover of the equatorial bulge at this longitude (125°W) compared to the two bulges reaching 400 m to the east and 500 m to the west (Fig. 1). Although sediment deficit has been observed further west (135–140°W, 5–7°N), where erosion has exposed Tertiary chalk and thus removed a substantial volume of sediment (Johnson, 1972; Marcantonio et al., 2001), this would have occurred too late to account for the Oligocene–Miocene sediment anomaly in Transect 5.

6.2. Sedimentation pattern

Pelagic sedimentation in the equatorial Pacific has been described by two models, "pelagic drape" and "basin fill" (see short review by Laguros and Shipley, 1989). Pelagic drape is the even settling of sediment through the water column throughout a region. It ignores topography so that equal amounts of sediment are deposited evenly on hills and in basins. Basin fill is the process whereby sediment is either preferentially deposited or subsequently reworked into topographic lows (basins), as found in many fossil pelagic depositional systems (see e.g. Santantonio, 1993, 1994). Examples of physical processes leading to the infilling of topography include quiescent flow (Flood, 1988; Mitchell and Hutnance, 2007) and diffusion (Mitchell, 1995; Webb and Jordan, 2001). Drape and fill can also act simultaneously, creating a more complex sediment configuration.

Tominaga et al. (2011) evaluated different stages of basin filling in AMAT03 by studying the radii of circular arcs fitted to seismic horizons from the basement to the seafloor. An increase in the radius indicates a flattening of the seafloor topography and preferential infilling of the basin. These authors suggest that depositional (east of U1337) and transitional (from U1337 to U1336) sedimentation regimes generally symmetrically drape the underlying basement within basins but have a somewhat subdued topography, whereas minimal sedimentation regimes (west of U1336) have more sedimentation within topographic lows and a more important seafloor relief.

We evaluated evidence for horizontal transport on the 100–1000 km scale and preferential basin filling processes (sediment focusing) by comparing the basement and seafloor depth along each transect. We used variations in sediment thickness as

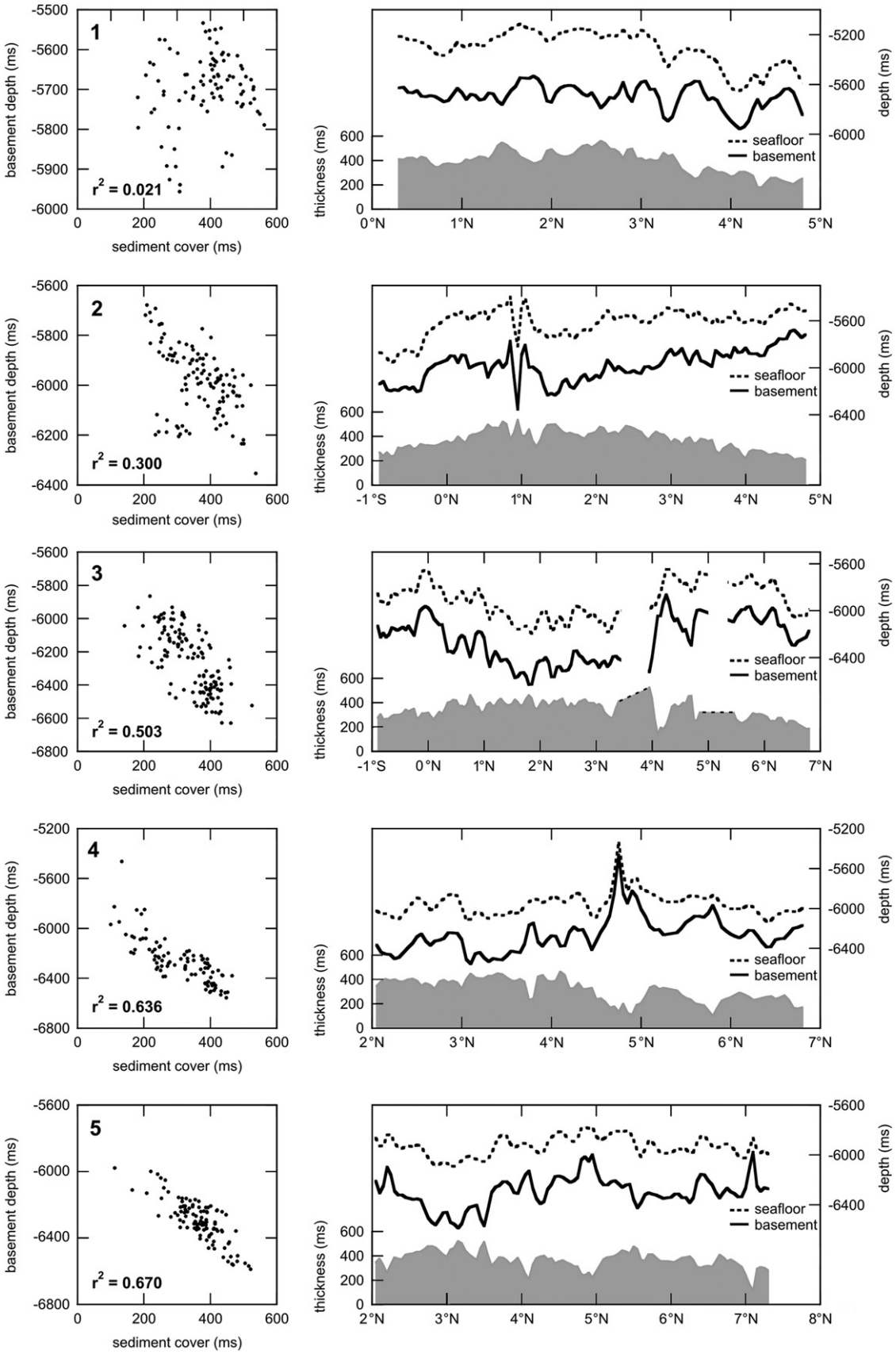

Fig. 7. Left column: Scatter plots of the basement depth in TWTT (ms) versus sediment thickness in TWTT (ms) for Transects 1–5 (top to bottom). Right column: Basement (black line) and seafloor (dotted line) depth in TWTT (ms) along Transects 1–5 (top to bottom), smoothed with a simple boxcar filter of full width 0.1° of latitude. Sediment thickness in TWTT (ms) is shown in gray at the bottom of each panel.

expressions of sediment redistribution. This simple approach is only a first order comparison of the basement depth and thickness of sediment layer in TWTT. It slightly underestimates the basement topography because acoustic velocity increases with sediment depth, but the error is likely to be small, based on the velocities reported by Pälike et al. (2010). A sediment pattern typical of "pelagic drape" lies conformably on basement, and thus should not reveal any relationship between basement depth and sediment cover. Sediment pattern typical of "basin fill" on the other hand is expected to reveal an inverse relationship between basement depth and sediment cover (larger cover in deeper basins). Fig. 7 illustrates these relationships along the five Transects. The scatter plots on the left of Fig. 7 reveal an increasingly stronger relationship between basement depth and sediment cover from east to west (Transect 1–5, with r^2 of 0.021, 0.3, 0.503, 0.636 and 0.670, respectively), with deeper basement corresponding to larger sediment thickness. The relationship illustrated in the scatter plots only works if the basement depth has no trend. In our case, only the results from Transect 2 should be considered with caution as the basement depth rises northward. The profiles on the right of Fig. 7 show the seafloor and basement depth along with the sediment thickness for each transect.

Fig. 7 therefore indicates a progressive departure from pelagic drape towards the western part of the studied area. In Transects 3–5 the thickest sediment cover is associated with deep basement elevations, and the thinnest sediment is associated with shallowest basins. Preferential infilling of abyssal valleys indicating higher sediment focusing and thus stronger currents and enhanced resuspension or sediment susceptibility to suspension become more significant in the western transects. Interestingly, the westernmost Transect 5 is also where the large-scale contourite is located and where most erosional features have been observed. The sedimentation style appears to revert back to basin-fill at the far east of the surveyed area (110°W, see Fig. 17 by Bloomer et al., 1995).

The results of our study indicate that the sedimentation pattern on a scale of hundred to thousand kilometers is more complex than what the simple conceptual model for pelagic environments would predict. Seafloor erosion and/or focusing, recent and ancient, have sculptured the sedimentary deposits both on local and regional scales. Over larger scales, the simple basin to hill redistribution process is insignificant compared with other sedimentological processes that are redistributing a significant part of the pelagic sediments.

7. Conclusion

The erosional features, basin-fill type sedimentation and contourite observed in the westernmost part of our study area emphasize that there is and has been significant redeposition of sediments within the central Pacific, suggesting conditions on the abyssal seafloor far from quiescent on timescales of millions of years.

We suggest that the large-scale excess of sediment has been eroded from the central part of the equatorial sediment bulge, where a sediment-deficient area creates a valley between two peaks in sediment thickness. Bottom currents have thus significantly influenced the sediment distribution pattern in this region, shaping the equatorial bulge. However, we cannot dismiss focusing as a significant contributor to the surplus of sediment observed in the western transect. Paleoceanographic results would be more accurate if drill sites were located as far as possible from areas of redeposition, in particular mass accumulation rates studies should take into account larger-scale sediment displacements as highlighted in this study.

Acknowledgments

We thank the captain and crew of R/V *Revelle*, Mitch Lyle and the shipboard scientists, as well as shipboard geophysical service from Scripps Institution of Oceanography for the data collected during the AMAT03 cruise. This study would not have been possible without the efforts of Christophe Serié, who kindly and generously shared endless expertise in seismic interpretation. A. Malinverno and T. Williams are thanked for discussions on the seismic data. This research is supported by NERC grant NE/C508985/2. Data acquisition was also supported by NSF grant OCE-9634141.

Appendix A. Supplementary material

Supplementary data associated with this article can be found in the online version at http://dx.doi.org/10.1016/j.dsr.2012.07.006.

References

Beaulieu, S.E., 2003. Resuspension of phytodetritus from the sea floor: a laboratory flume study. Limnol. Oceanogr. 48, 1235–1244.

Berger, W.H., Adelseck, C.G., Mayer, L.A., 1976. Distribution of carbonate in surface sediments of the Pacific Ocean. J. Geophys. Res. 81, 2617–2627, http://dx.doi.org/10.1029/JC081i015p02617.

Berger, W.H., Bonneau, M.-C., Parker, F.L., 1982. Foraminifera on the deep-sea floor: lysocline and dissolution rate. Oceanol. Acta 5, 249–258.

Bloomer, S.F., Mayer, L.A., Moore Jr., T.C., 1995. Seismic stratigraphy of the eastern equatorial Pacific Ocean: Paleoceanographic implications. Proc. Ocean Drill. Program Sci. Results 138, 537–553, http://dx.doi.org/10.2973/odp.proc.sr.138.128.1995.

Broecker, W., 2008. Excess sediment ^{230}Th: transport along the sea floor or enhanced water column scavenging? Global Biogeochem. Cycles 22, GB003057, GB1006, http://dx.doi.org/10.1029/2007.

Divins, D.L., 2012. NGDC Total Sediment Thickness of the World's Oceans & Marginal Seas, Retrieved date goes here, 〈http://www.ngdc.noaa.gov/mgg/sedthick/sedthick.html〉.

Ewing, J., Ewing, M., Aitken, T., Ludwig, W.J., 1968. North Pacific sediment layers measured by seismic profiling. In: Knopoff, L., Drake, C.L., Hart, P.J. (Eds.), The Crust and Upper Mantle of the Pacific Area. American Geophysical Union. Geophysical Monograph 12, pp. 147–186.

Farrell, J.W., Prell, W.L., 1989. Climatic change and $CaCO_3$ preservation: an 800,000 year bathymetric reconstruction from the central equatorial Pacific Ocean. Paleoceanography 4, 447–466, http://dx.doi.org/10.1029/PA004i004p00447.

Feely, R.A., Sabine, C.L., Lee, K., Berelson, W., Kleypas, J., Fabry, V.J., Millero, F.J., 2004. Impact of anthropogenic CO_2 on the $CaCO_3$ system in the oceans. Science 305, 362–366.

Feely, R.A., Sabine, C.L., Lee, K., Millero, F.J., Lamb, M.F., Greeley, D., Bullister, J.L., Key, R.M., Peng, T.-H., Kozyr, A., Ono, T., Wong, C.S., 2002. In situ calcium carbonate dissolution in the Pacific Ocean. Global Biogeochem. Cycles 16, http://dx.doi.org/10.1029/2002GB001866.

Flood, R.D., 1988. A lee wave model for deep-sea mudwave activity. Deep-Sea Res. 35, 973–983.

François, R., Frank, M., Rutgers van der Loeff, M., Bacon, M.P., Geibert, W., Kienast, S.S., Anderson, R.F., Bradtmiller, L.I., Chase, Z., Henderson, G.M., Marcantonio, F., Allen, S.E., 2007. Comment on "Do geochemical estimates of sediment focusing pass the sediment test in the equatorial Pacific?" by M. Lyle et al.. Paleoceanography 22, PA1216, http://dx.doi.org/10.1029/2005PA001235.

François, R., Frank, M., Rutgers van der Loeff, M.M., Bacon, M.P., 2004. ^{230}Th normalization: an essential tool for interpreting sedimentary fluxes during the late Quaternary. Paleoceanography 19, PA1018, http://dx.doi.org/10.1029/2003PA000939.

Higgins, S.M., Broecker, W.S., Anderson, R.F., McCorkle, D.C., Timothy, D., 1999. Enhanced sedimentation along the equator in the western Pacific. Geophys. Res. Lett. 26, 3489–3492.

Johnson, D.A., 1972. Ocean-floor erosion in the Equatorial Pacific. Geol. Soc. Am. Bull. 83, 3121–3144.

Johnson, D.A., Johnson, T.C., 1970. Sediment redistribution by bottom currents in the central Pacific. Deep-Sea Res. 17, 157–169.

Kienast, S.S., Kienast, M., Mix, A.C., Calvert, S.E., François, R., 2007. Thorium-230 normalized particle flux and sediment focusing in the Panama Basin region during the last 30,000 years. Paleoceanography 22, PA2213.

Knappenberger, M.B., 2000. Sedimentation Rates and Pacific Plate Motion Calculated Using Seismic Cross Sections of the Neogene Equatorial Sediment Bulge. M.S. Thesis. Boise State University, Boise, Idaho, 95 pp.

Koppers, A.A.P., Phipps Morgan, J., Morgan, W.J., Staudigel, H., 2001. Testing the fixed hotspot hypothesis using ^{40}Ar/^{39}Ar age progressions along seamount

trails. Earth Planet. Sci. Lett. 185, 237–252, http://dx.doi.org/10.1016/S0012-821X(00)00387-3.
Laguros, G.A., Shipley, T.H., 1989. Quantitative estimate of resedimentation in the pelagic sequence of the equatorial Pacific. Mar. Geol. 89, 269–277.
Loubere, P., Mekik, F., François, R., Pichat, S., 2004. Export fluxes of calcite in the eastern equatorial Pacific from the Last Glacial Maximum to present. Paleoceanography 19, PA2018, http://dx.doi.org/10.1029/2003PA000986.
Lyle, M., 2003. Neogene carbonate burial in the Pacific Ocean. Paleoceanography 18 , http://dx.doi.org/10.1029/2002PA000777.
Lyle, M., Dadey, K.A., Farrell, J.W., 1995. The late Miocene (11–8 Ma) eastern Pacific carbonate crash: evidence for reorganization of deep-water circulation by the closure of the Panama Gateway. Proc. Ocean Drill. Program Sci. Results 138, 821–838, http://dx.doi.org/10.2973/odp.proc.sr.138.157.1995.
Lyle, M., Mitchell, N., Pisias, N., Mix, A., Martinez, J.I., Paytan, A., 2005. Do geochemical estimates of sediment focusing pass the sediment test in the equatorial Pacific? Paleoceanography 20, PA1005, http://dx.doi.org/10.1029/2004PA001019.
Lyle, M., Pälike, H., Nishi, H., Raffi, I., Gamage, K., Klaus, A., the IODP Expeditions 320/321 Scientific Party, 2010. The Pacific Equatorial Age Transect, IODP Expeditions 320 and 321: building a 50-million-year-long environmental record of the equatorial Pacific Ocean. Sci. Drill. 9, 4–15, http://dx.doi.org/10.2240/iodp.sd.9.01.2010.
Lyle, M., Pisias, N., Paytan, A., Martinez, J.I., Mix, A., 2007. Reply to comment by R. François et al. on "Do geochemical estimates of sediment focusing pass the sediment test in the equatorial Pacific?": further explorations of ^{230}Th normalization. Paleoceanography 22, PA1217, http://dx.doi.org/10.1029/2006PA001373.
Lyle, M.W., Pälike, H., Moore, T.C., Mitchell, N., Backman, J., 2006. Summary Report of R/V *Roger Revelle* Site Survey AMAT03 to the IODP Environmental Protection and Safety Panel (EPSP) in Support for Proposal IODP626. University of Southampton), Southampton, UK 〈http://eprints.soton.ac.uk/45921/〉.
Marcantonio, F., Anderson, R.F., Higgins, S., Stute, M., Schlosser, P., Kubik, P., 2001. Sediment focusing in the central equatorial Pacific Ocean. Paleoceanography 16, 260–267, http://dx.doi.org/10.1029/2000PA000540.
Mayer, L., Theyer, F., et al., 1985b. Initial Reports Deep-Sea Drilling Project 85 1021 pp.
Mayer, L.A., 1991. Extraction of high-resolution carbonate data for palaeoclimate reconstruction. Nature 352, 148–150, http://dx.doi.org/10.1038/352148a0.
Mayer, L.A., Shipley, T.H., Theyer, F., Wilkens, R.H., Winterer, E.L., 1985a. Seismic modeling and paleoceanography at deep sea drilling project Site 574. Deep Sea Drill. Proj. 85, 947–970.
Mayer, L.A., Shipley, T.H., Winterer, E.L., 1986. Equatorial Pacific seismic reflectors as indicators of global oceanographic events. Science 233, 761–764, http://dx.doi.org/10.1126/science.233.4765.761.
McManus, J.F., Oppo, D.W., Cullen, J.L., 1999. A 0.5-million-year record of millennial-scale climate variability in the North Atlantic. Science 283, 971–975, http://dx.doi.org/10.1126/science.283.5404.971.
Menard, H.W., 1964. Marine Geology of the Pacific. McGraw-Hill, New York 271 pp.
Mitchell, N.C., 1995. Diffusion transport model for pelagic sediments on the Mid-Atlantic Ridge. J. Geophys. Res. 100, 19,991–20,009.
Mitchell, N.C., 1998. Modeling Cenozoic sedimentation in the central equatorial Pacific and implications for true polar wander. J. Geophys. Res. 103, 17,749–17,766.
Mitchell, N.C., Hutnance, J.M., 2007. Comparing the smooth, parabolic shapes of interfluves in continental slopes to predictions of diffusion transport models. Mar. Geol. 236, 189–208.
Mitchell, N.C., Lyle, M.W., 2005. Patchy deposits of Cenozoic pelagic sediments in the central Pacific. Geology *33* (1), 49.
Mitchell, N.C., Lyle, M.W., Knappenberger, M.B., Liberty, L.M., 2003. Lower Miocene to present stratigraphy of the equatorial Pacific sediment bulge and carbonate dissolution anomalies. Paleoceanography 18 (2), 1038, http://dx.doi.org/10.1029/2002PA000828.
Mollenhauer, G., Kienast, M., Lamy, F., Meggers, H., Schneider, R.R., Hayes, J.M., Eglinton, T.I., 2005. An evaluation of 14C age relationships between co-occurring foraminifera, alkenones, and total organic carbon in continental margin sediments. Paleoceanography 20, PA1016, http://dx.doi.org/10.1029/2004PA001103.
Nodder, S.E., Duineveld, G.C.A., Pilditch, C.A., Sutton, P.J., Probert, P.K., Lavaleye, M.S.S., Witbaard, R., Chang, F.H., Hall, J.A., Richardson, K.M., 2007. Focusing of phytodetritus deposition beneath a deep-ocean front, Chatham Rise, New Zealand. Limnol. Oceanogr. 52, 299–314.
Ohkouchi, N., Eglinton, T.I., Keigwin, L.D., Hayes, J.M., 2002. Spatial and temporal offsets between proxy records in a sediment drift. Science 298, 1224–1227.
Pälike, H., Lyle, M., Nishi, H., Raffi, I., Gamage, K., Klaus, A., and the Expedition 320/321 Scientists, 2010. Proceedings of the Integrated Ocean Drilling Program 320/321. 10.2204/iodp.proc.320321.101.2010.
Pälike, H., Lyle, M.W., Ahagon, N., Raffi, I., Gamage, K., Zarikian, C.A., 2008. Pacific equatorial age transect (online). Integrated Ocean Drill. Program. Sci. Prospectus 320/321, 96, http://dx.doi.org/10.2204/iodp.sp.320321.2008.
Peterson, L.C., Haug, G.H., Murray, R.W., Yarincik, K.M., King, J.W., Bralower, T.J., Kameo, K., Rutherford, S.D., Pearce, R.B., 2000. Late Quaternary stratigraphy and sedimentation at Site 1002, Cariaco Basin (Venezuela). Proc. Ocean Drill. Program Sci. Results 165, 85–99, http://dx.doi.org/10.2973/odp.proc.sr.165.017.2000.
Peterson, M.N.A., 1966. Calcite: rates of dissolution in a vertical profile in the central Pacific. Science 154, 1542–1544.
Rebesco, M., 2005. Contourites. In: Selley, R.C., Cocks, L.R.M., Plimer, I.R. (Eds.), Encyclopedia of Geology, vol. 4. Elsevier, Oxford, pp. 513–527.
Santantonio, M., 1993. Facies associations and evolution of pelagic carbonate platform/basin systems: examples from the Italian Jurassic. Sedimentology 40, 1039–1067.
Santantonio, M., 1994. Pelagic carbonate platforms in the geologic record: their classification, and sedimentary and paleotectonic evolution. Am. Assoc. Petrol. Geol. Bull. 78, 122–141.
Shipley, T.H., Winterer, E.L., Goud, M., Mills, S.J., Metzler, C.V., Paull, C.K., Shay, J.T., 1985. Seabeam bathymetric and water-gun seismic reflection surveys in the equatorial Pacific. Initial Rep. Deep Sea Drill. Proj. 85, 825–837.
Smith, W.H.F., Sandwell, D.T., 1997. Global seafloor topography from satellite altimetry and ship depth soundings. Science 277, 1957–1962.
Southard, J.B., Young, R.A., Hollister, C.D., 1971. Experimental erosion of fine abyssal sediment. J. Geophys. Res. 76, 5903–5909.
Stow, D.A.V., Hunter, S., Wilkinson, D., Hernandez-Molina, F.J., 2008. The nature of contourite deposition. In: Rebesco, M., Camerlenghi A. (Eds.) Developments in Sedimentology, vol. 60, 143–156 (Chapter 9).
Stow, D.A.V., Ogawa, Y., Lee, I.T., Mitsuzawa, K., 2002. Neogene contourites, Miura-Boso forearc basin, SE Japan. In: Stow, D.A.V., Pudsey, C.J., Howe, J.A., Fauge'res, J.-C., Viana, A.R. (Eds.), Deep-Water Contourite Systems: Modern Drifts and Ancient Series, Seismic and Sedimentary Characteristics. Geological Society of London Memoirs, vol. 22, pp. 409–419.
Thiede, J., 1981. Reworking in Upper Mesozoic and Cenozoic central Pacific deep-sea sediments. Nature 289, 667–670.
Tominaga, M., Lyle, M., Mitchell, N.C., 2011. Seismic interpretation of pelagic sedimentation regimes in the 18–53 Ma eastern equatorial Pacific: basin-scale sedimentation and infilling of abyssal valleys. Geochem. Geophys. Geosyst. 12, Q03004, http://dx.doi.org/10.1029/2010GC003347.
van Andel, T.H., Moore, T.C., 1974. Cenozoic migration of the Pacific plate, northward shift of the axis of deposition, and paleobathymetry of the central equatorial Pacific. Geology 2, 507–510, http://dx.doi.org/10.1130/0091-7613(1974)2 $<$507:CMOTPP$>$2.0.CO;2.
van Andel, T.J., Heath, G.R., Moore, T.C., 1975. Cenozoic Tectonics, Sedimentation, and Paleoceanography of the Central Equatorial Pacific. Geological Society of America, Boston, MA, 134 pp.
Webb, H.F., Jordan, T.H., 2001. Pelagic sedimentation on rough seafloor topography: 1. Forward Model. J. Geophys. Res. 106, 30,433–30,444.